

## TORQUE-RIPPLE MINIMIZATION FOR SWITCHED RELUCTANCE MOTOR BASED ON TORQUE SHARING FUNCTION BY FUZZY VARIABLE ANGLE STRATEGY

ZHANQIAN LIU<sup>1,2</sup>, YANXIANG YANG<sup>2,\*</sup>, JUN WANG<sup>1,2</sup>  
XIAOXIAO SONG<sup>1,2</sup> AND JING TANG<sup>1,2</sup>

<sup>1</sup>Sichuan Province Key Laboratory of Power Electronics Energy-Saving Technologies and Equipment

<sup>2</sup>School of Electrical Engineering and Electronic Information  
Xihua University

No. 999, Jinzhou Road, Jinniu District, Chengdu 610039, P. R. China

\*Corresponding author: 672291877@qq.com

Received June 2016; accepted September 2016

**ABSTRACT.** *Switched reluctance motors (SRMs) have salient torque ripple due to its doubly salient poles and non-linear magnetic characteristic. Aiming at the large torque ripple of SRM in conventional control method, a fuzzy variable angle control method is presented based on torque sharing function (TSF) in this paper. Automatic adjustment of the turn-on angle and turn-off angle is adopted and the torque ripple is reduced effectively. The effectiveness of the proposed method is validated through the simulation and experimental results.*

**Keywords:** Switched reluctance motor, Torque sharing function, Fuzzy control, Torque ripple minimization

**1. Introduction.** Switched reluctance motor (SRM) is a new type of motor. It has great development potential for its simple and robust structure, wide speed range, flexible control system and high reliability. However, it was not successful in its wide use due to its serious instantaneous torque ripple. The torque ripple is caused by its doubly salient structure and the characteristic of high nonlinearity of the magnetic properties. Furthermore, the torque ripple is more severe than these of other traditional motors [1-3]. Hence, how to suppress the torque ripple of SRM is a hot spot of research.

The torque ripple of SRM is more serious during the phase winding current commutation [4,5]. The conventional control strategies, such as current chopper control (CCC) and angular position control (APC), could not suppress torque ripple effectively because the smooth transition of torque is not considered [6-8]. In recent years, some researchers have applied the torque sharing function (TSF) to the torque control of SRM. An optimized TSF was proposed based on the minimization of copper consumption and current rate of change in [9,10]. Similarly, a new torque-sharing control strategy for minimizing the torque tracking error was presented in [11]. In the meanwhile, the method of compensating phase torque by increasing or decreasing other phases current based on TSF was proposed in [12]. Although the control effect is obtained in the above schemes, the effect of torque-sharing is not good due to the fixed turn-on angle and turn-off angle.

In this paper, a variable angle control strategy based on TSF is presented for minimizing the torque ripple. In view of the high nonlinearity of SRM, we combine the control strategy with fuzzy control in order to achieve the automatic adjustment of the turn-on angle and turn-off angle. Therefore, the torque ripple is reduced effectively. An experiment platform of a 3-phase, 12/8-pole SRM is set up. The proposed method is adopted in controlling the SRM.

The remaining part of the paper is organized as follows. The cosine TSF and the structure of the control system of SRM are introduced in Section 2. The effect of turn-on angle and turn-off angle on the performance of SRM is described in Section 3. The design of the fuzzy controller with variable turn-on angle and turn-off angle is introduced in Section 4. The simulation and experimental results are presented in Section 5. Conclusions are drawn in Section 6.

## 2. The Control System of SRM Based on TSF.

**2.1. The structure of control system.** In SRM drive, the information about rotor position is essential for the proper switching operation [13,14]. When the angle of the rotor position matches the turn-on angle, the phase switches are turned on. Then phase current starts to be built up. Similarly, phase switches are turned off when the angle of the rotor position matches the turn-off angle. Hence, the power source will stop to input energy.

Figure 1 shows the control system block diagram of TSF method. The fixed turn-on angle and turn-off angle are adopted in conventional TSF. The reference torque ( $T^*$ ) is divided into target torque for three-phase ( $T_k^*$ ) by the block of TSF. Meanwhile, the target torque of each phase is changed to target current signal ( $I_k^*$ ) by the block of *Torque-to-Current*. The block of *Torque-to-Current* is a static lookup table, and its inputs are rotor position ( $\theta$ ) and phase torque ( $T_k^*$ ). The lookup table is obtained from off-line inversion operation, formed from static measured torque at different rotor positions and phase currents. According to the current error, the switching rule generates an active switching signal ( $S_k$ ) to power inverter. Then the SRM is driven by the power inverter.

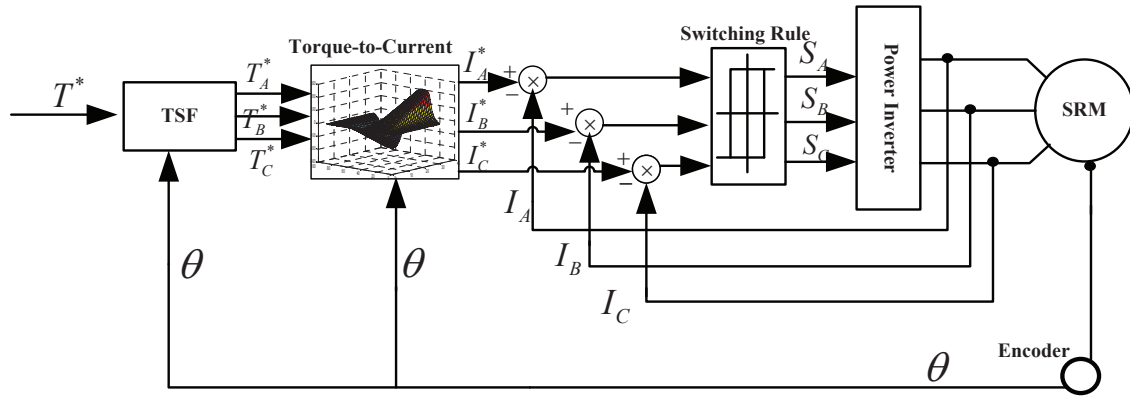


FIGURE 1. The block diagram of the control system with TSF method

**2.2. Torque sharing function.** Target torque of each phase in different rotor positions is assigned by TSF. Therefore, the output of synthetic torque will track the target torque waveform with a small error. The cosine TSF is adopted in the control system and its curve is shown as Figure 2. In the cosine TSF, the target torque of each phase is defined as follows

$$\begin{cases} T_k^* = f_k(\theta)T^* \\ \sum_{k=1}^3 f_k(\theta) = 1 \end{cases} \quad (1)$$

where  $f_k(\theta)$  is the TSF for phase  $k$ ,  $T_k^*$  is the target torque for phase  $k$ ,  $T^*$  is the reference torque, and  $\theta$  is the angle of the rotor position. The mechanical angle of the total length of one cycle is 45 degrees. In one cycle, the target torque of each phase can be expressed

as follows

$$T_k^* = \begin{cases} 0 & 0 \leq \theta \leq \theta_{on} \\ \frac{T^*}{2} - \frac{T^*}{2} \cos \frac{\pi}{\theta_{ov}} (\theta - \theta_{on}) & \theta_{on} \leq \theta \leq \theta_{on} + \theta_{ov} \\ T^* & \theta_{on} + \theta_{ov} \leq \theta \leq \theta_{off} \\ \frac{T^*}{2} + \frac{T^*}{2} \cos \frac{\pi}{\theta_{ov}} (\theta - \theta_{off}) & \theta_{off} \leq \theta \leq \theta_{off} + \theta_{ov} \\ 0 & \theta_{off} + \theta_{ov} \leq \theta \leq \tau \end{cases} \quad (2)$$

where  $\theta_{on}$  is the turn-on angle,  $\theta_{off}$  is the turn-off angle,  $\theta_{ov}$  is the angle of overlapping interval, and  $\tau$  is the angle of the cycle.

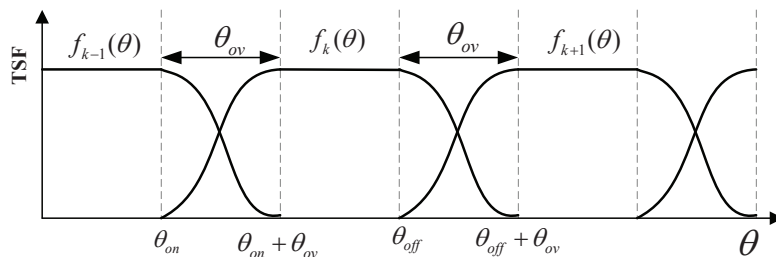


FIGURE 2. The curve of cosine TSF

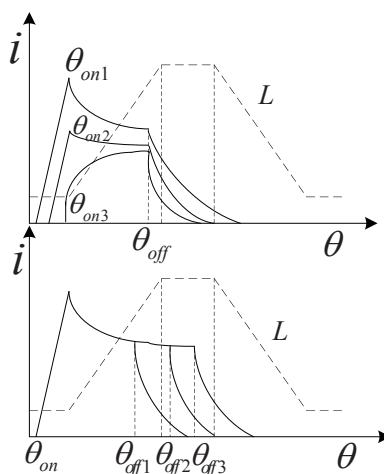


FIGURE 3. The current curves in different turn-on angle and turn-off angle

**3. The Effect of Turn-on Angle and Turn-off Angle on the Performance of SRM.** The turn-on angle and turn-off angle are important parameters, which influence the SRM torque ripple remarkably. Figure 3 shows the current curves in different turn-on angles and turn-off angles. The dotted line is inductance value ( $L$ ). In order to obtain sufficient torque for SRM, the phase current should be established quickly. Therefore, the motor needs to be driven at the minimum inductance value. Once the free-wheeling of the phase winding flows into the inductance drop zone, brake torque would be generated and the torque ripple would be increased. Thus, the motor needs to be shut off before reaching the maximum inductance value.

While the turn-off angle is fixed, the curves of torque and current in different turn-on angles are shown in Figure 4. According to the analysis of Figure 3, the phase current could not be established quickly if the turn-on angle is larger. When the torque is insufficient, the torque ripple is remarkable. The torque ripple could be effectively suppressed if the

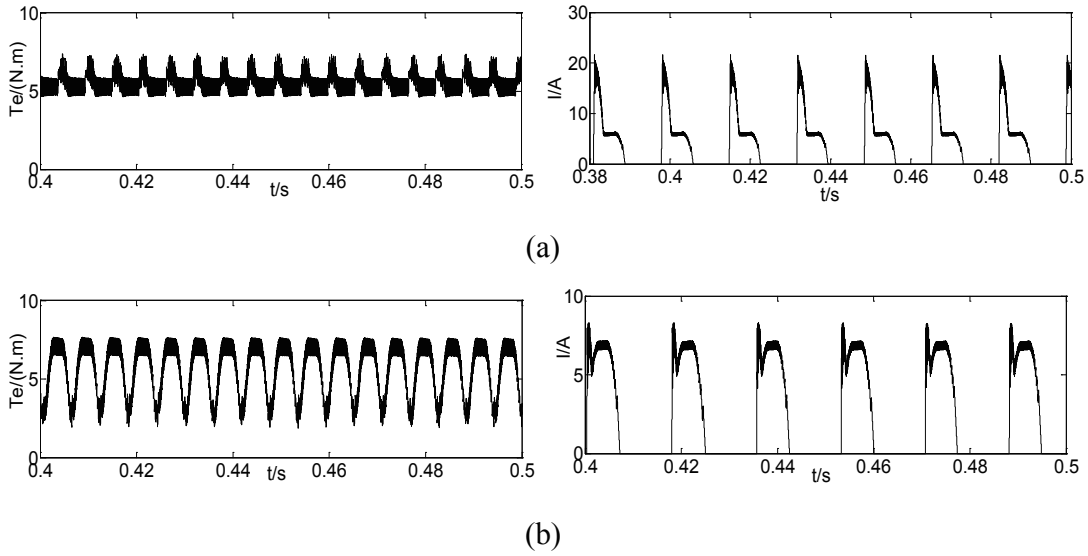


FIGURE 4.  $\theta_{off}$  is 15 degrees: (a)  $\theta_{on}$  is  $-1$  degree, (b)  $\theta_{on}$  is 3 degrees.

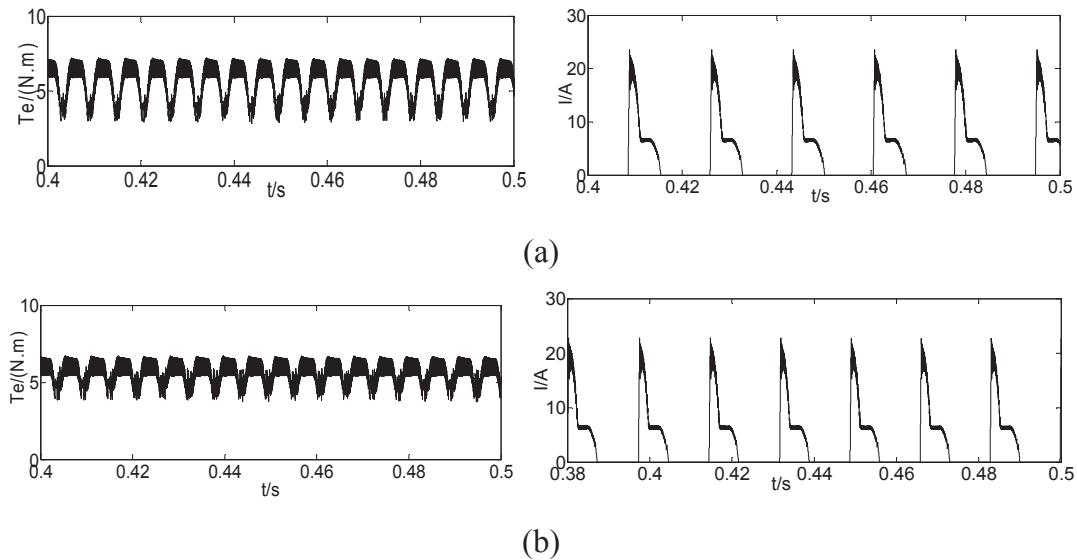


FIGURE 5.  $\theta_{on}$  is  $-1$  degree: (a)  $\theta_{off}$  is 12 degrees, (b)  $\theta_{off}$  is 13 degrees.

turn-on angle is reduced properly. However, the smaller turn-on angle could cause larger impulse current and the torque ripple would be increased.

While the turn-on angle is fixed, the curves of torque and current in different turn-off angles are shown in Figure 5. According to the analysis of Figure 3, the peak value of the phase current does not change while the turn-off angle is changed. The torque ripple could be effectively suppressed if the turn-off angle is increased in a certain range. However, while the turn-off angle is larger, the brake torque is generated because the free-wheeling of the phase winding flows into the braking area. Hence, the torque ripple would be increased and the efficiency of SRM could be reduced as well.

From the above analysis, it could be seen that the change of the turn-on angle and turn-off angle has great influence on the torque ripple. When the speed and load change, the system could not obtain a better control effect with fixed turn-on angle and turn-off angle. Therefore, the method which adopts the variable turn-on angle and turn-off angle is proposed in this paper.

**4. The Design of the Fuzzy Controller with Variable Turn-on Angle and Turn-off Angle.** The rotor angle of SRM has stronger nonlinear relationship with the corresponding torque and current. Thus, the accurate mathematical expression is hard to establish.

Fuzzy control is a kind of nonlinear control with strong robustness and adaptability [14-16]. In this paper, fuzzy logic is used to optimize the turn-on angle and turn-off angle. The method realizes the automatic adjustment of the turn-on angle and turn-off angle in the process of operation.

Figure 6 shows the control system block diagram based on the fuzzy controller with variable turn-on angle and turn-off angle. The speed error ( $e$ ) is changed to the reference torque ( $T^*$ ) by the PI controller. The variable turn-on angle ( $\theta_{on}$ ) and turn-off angle ( $\theta_{off}$ ) are obtained by the fuzzy controller. The fuzzy controller input variables include speed error ( $e$ ) and speed error derivative ( $e_c$ ). The variable turn-on angle and turn-off angle are adopted in the improved TSF.

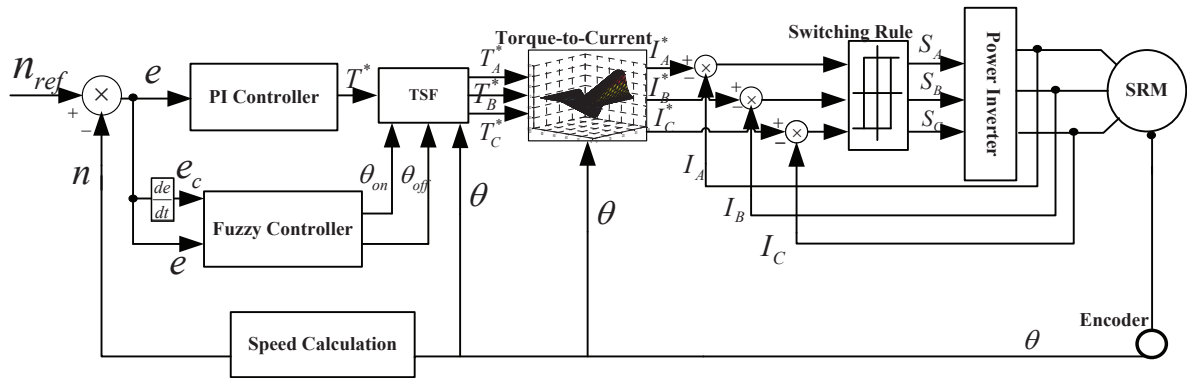


FIGURE 6. The block diagram of the control system based on the fuzzy controller

The input variables of the fuzzy controller are speed error ( $e$ ) and speed error derivative ( $e_c$ ), and the output variables are the variation of turn-on angle ( $\Delta\theta_{on}$ ) and turn-off angle ( $\Delta\theta_{off}$ ). The basic domain of speed error and speed error derivative is  $[-1000, 1000]$ . The fuzzy domain of input ( $e, e_c$ ) and output ( $\Delta\theta_{on}, \Delta\theta_{off}$ ) is  $\{-3, -2, -1, 0, 1, 2, 3\}$ .

The triangular membership function is adopted in this paper. The fuzzy subsets of linguistic variable are negative big ( $NB$ ), negative small ( $NS$ ), zero ( $ZO$ ), positive small ( $PS$ ), positive big ( $PB$ ). According to practical experience, the fuzzy rule tables could be established [17]. The fuzzy rule tables about  $\Delta\theta_{on}$  and  $\Delta\theta_{off}$  are shown in the following.

TABLE 1. Fuzzy rule table of  $\Delta\theta_{on}$

$e \backslash e_c$	$NB$	$NS$	$ZO$	$PS$	$PB$
$NB$	$PB$	$PS$	$PS$	$PS$	$ZO$
$NS$	$PS$	$PS$	$ZO$	$ZO$	$NS$
$ZO$	$PS$	$PS$	$ZO$	$NS$	$NS$
$PS$	$PS$	$ZO$	$NS$	$NS$	$NB$
$PB$	$ZO$	$NS$	$NS$	$NB$	$NB$

TABLE 2. Fuzzy rule table of  $\Delta\theta_{off}$

$e \backslash e_c$	$NB$	$NS$	$ZO$	$PS$	$PB$
$NB$	$NB$	$NB$	$NS$	$NS$	$ZO$
$NS$	$NB$	$NS$	$NS$	$ZO$	$PS$
$ZO$	$NS$	$NS$	$ZO$	$PS$	$PS$
$PS$	$NS$	$ZO$	$PS$	$PS$	$PB$
$PB$	$ZO$	$PS$	$PS$	$PB$	$PB$

In order to realize the dynamic definition of the turn-on angle and turn-off angle, the weighted average method is adopted to achieve defuzzification. The dynamic parameters ( $\theta_{on}, \theta_{off}$ ) are taken to the following expression

$$\theta_{on} = \theta_{on1} + \Delta\theta_{on} \quad (3)$$

$$\theta_{off} = \theta_{off1} + \Delta\theta_{off} \quad (4)$$

where  $\theta_{on1}$  is the turn-on angle reference, and  $\theta_{off1}$  is the turn-off angle reference.

## 5. Simulations and Experimental Results.

**5.1. Simulations.** According to the above control strategy, the model of the control system for SRM is built in Matlab/Simulink. The main parameters of the experimental motor are as follows: number of stators and rotor poles are 12 and 8, rated power is 11 kW, resistance of stator winding is 0.05  $\Omega$ , and rotor inertia is 0.05 kg·m<sup>2</sup>.

The reference speed is 500 r/min, and the load is 5 N·m. Figure 7 shows the curves of torque and current in steady-state process. Compared with Figure 4 and Figure 5, the torque ripple is suppressed effectively by using the improved TSF with fuzzy logic.

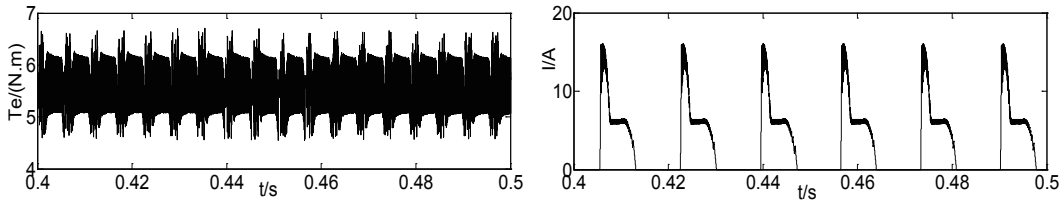


FIGURE 7. The curves of torque and current

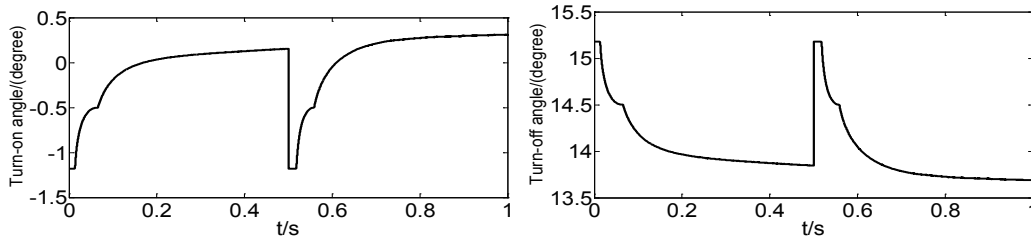


FIGURE 8. The curves of the turn-on angle and turn-off angle

When the reference speed is changed to 1000 r/min at 0.7 s, the turn-on angle should be smaller and the turn-off angle should be larger in order to obtain enough power. Figure 8 shows the curves of the turn-on angle and turn-off angle. With the increasing of the rotor speed, the turn-on angle increases so that the impulse current could be reduced effectively. Meanwhile, the turn-off angle decreases so that the free-wheeling of the phase winding which flows into the braking area could be reduced. Therefore, the torque ripple is suppressed significantly.

Figure 9 shows the contrast curves of torque in the steady-state process between the conventional TSF and the improved TSF. Compared with the conventional TSF with the fixed turn-on angle and turn-off angle, the torque ripple of the improved TSF with the fuzzy variable angle is reduced by about 3.4%.

**5.2. Experimental results.** In order to verify the effectiveness of the proposed method, the experiment platform of a 3-phase, 12/8-pole SRM is set up. The experiment devices are shown in Figure 10. It includes SRM, dynamometer and hardware circuits of a digital control system based on TMS320F2812.

Figure 11 shows the measured waveform of current for phase A. It coincides with the simulation result. Figure 12 shows the contrast curves of the measured torque. The torque ripple is suppressed effectively by the improved TSF with fuzzy logic. From Figure 11 and Figure 12, we can conclude that the proposed method is reasonable and effective.

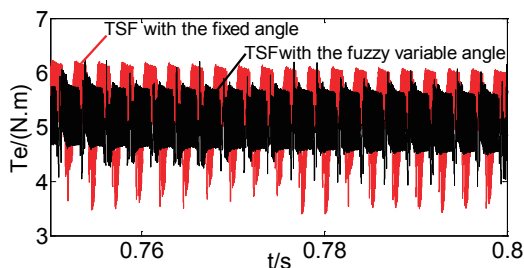


FIGURE 9. The contrast curves of torque

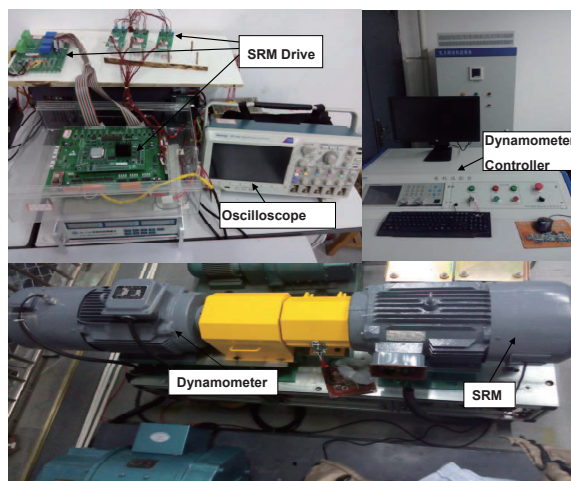


FIGURE 10. The experimental devices

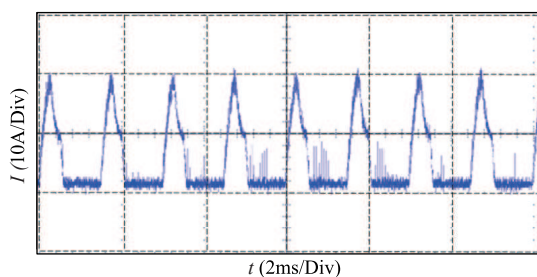


FIGURE 11. The measured waveform of current for phase A

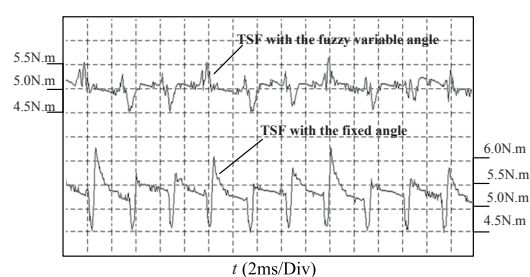


FIGURE 12. The contrast curves of the measured torque

**6. Conclusions.** In this paper, a variable angle control strategy based on TSF is presented for minimizing the torque ripple. In view of the high nonlinearity of SRM, fuzzy logic is used to optimize the turn-on angle and turn-off angle. It realizes the automatic adjustment of the turn-on angle and turn-off angle in the process of operation. Compared with the conventional TSF with the fixed turn-on angle and turn-off angle, the inhibition effect of torque ripple with the improved TSF is more significant. The simulation and experimental results show that the proposed method is reasonable and effective.

The fuzzy rule tables adopted in this paper are established based on practical experience. For the better control performances, the fuzzy rule tables should be further optimized. This would be the focus of our future research.

**Acknowledgment.** This work is supported by Sichuan Provincial Department of Science and Technology (Grant No. 14ZC2277, Grant No. 2015GZ0060), the Opening Fund of the Key Laboratory of Sichuan Province (Grant No. szjj2015065) and the Innovation Fund of Postgraduate of Xihua University (Grant No. ycyj2015211).

**REFERENCES**

- [1] A. Hellany, M. Nagrial, W. Aljaim and J. Rizk, Analysis design optimisation and simulation of switched reluctance motors, *IEEE Conference on Energy Conversion*, pp.134-139, 2014.
- [2] C. Moron, A. Garcia and E. Tremps, Torque control of switched reluctance motors, *IEEE Trans. Magnetics*, vol.48, no.4, pp.1661-1664, 2012.
- [3] P. V. Vladan, Minimization of torque ripple and copper losses in switched reluctance drive, *IEEE Trans. Power Electronics*, vol.27, no.1, pp.388-399, 2012.
- [4] Z. Q. Liu, J. Tang, Y. X. Yang, J. Wang and X. X. Song, An improved direct torque control for switched reluctance motor based on fuzzy adaptive, *Small and Special Electrical Machines*, vol.44, no.5, pp.71-74, 2016.

- [5] A. Shahabi, A. Rashidi and A. Afshoon, Commutation angles adjustment in SRM drives to reduce torque ripple below the motor base speed, *Turkish Journal of Electrical Engineering and Computer Sciences*, vol.24, no.2, pp.669-682, 2016.
- [6] X. L. Wang and Z. L. Xu, Speed regulation control of switched reluctance motors based on PI parameter self-adaptation, *Proc. of the CSEE*, vol.35, no.16, pp.4215-4222, 2015.
- [7] J. Kim, K. Ha and R. Krishnan, Single-converters for switched reluctance motor drive for low cost, variable-speed applications, *IEEE Trans. Power Electronics*, vol.27, no.1, pp.47-59, 2010.
- [8] D. H. Kim, H. G. Jeong and K. B. Lee, Torque ripple minimization of switched reluctance motors based on fuzzy logic and sliding mode control, *IEEE International Symposium on Industrial Electronics*, pp.1-6, 2013.
- [9] X. D. Xue, K. W. Cheng and J. K. Lin, Optimal control method of motoring operation for SRM drives in electric vehicles, *IEEE Trans. Vehicular Technology*, vol.59, no.3, pp.1191-1204, 2010.
- [10] H. S. Ro, K. G. Lee, J. S. Lee, H. G. Jeong and K. B. Lee, Torque ripple minimization scheme using torque sharing function based fuzzy logic control for a switched reluctance motor, *Journal of Electrical Engineering and Technology*, vol.10, no.1, pp.118-127, 2015.
- [11] J. Y. Cao, H. Cai and W. Wang, A new torque control method for switched reluctance motors, *Journal of Chinese Electrical Engineering Science*, vol.25, no.6, pp.88-94, 2005.
- [12] X. Y. Chen and Y. X. Peng, Torque-ripple minimization for SRMs with segmental rotors and fully-pitched windings based on TSF by current compensation strategy, *Journal of Transactions of China Electrotechnical Society*, vol.1, no.29, pp.131-138, 2014.
- [13] J. W. Ahn, Switched reluctance motor, *Torque Control*, pp.201-252, 2011.
- [14] M. Divandari, B. Rezaie and B. Askari-Ziarati, Torque estimation of sensorless SRM drive using adaptive-fuzzy logic control, *IEEE NW Russia Young Researchers in Electrical and Electronic Engineering Conference*, pp.542-546, 2016.
- [15] A. Guettaf, F. Benchabane, M. Bahri and O. Bennis, Reduction of periodic speed ripples in switched reluctance motor using fuzzy logic control, *Power Electronics and Motion Control Conference and Exposition*, pp.305-310, 2014.
- [16] J. Wang, *Intelligent Control Technology of Permanent Magnet Synchronous Motor*, Southwest Jiao Tong University Press, Chengdu, 2015.
- [17] S. Y. Wang, F. Y. Liu, C. L. Tseng and J. H. Chou, Fuzzy inference of excitation angle for direct torque-controlled switched reluctance motor drives, *IEEE International Conference on Systems, Man, and Cybernetics*, pp.1139-1144, 2015.